Modelling of Lateral Dynamics for an Endless Metal Process Belt

Klemens. G. Schulmeister, Martin Kozek
Vienna University of Technology, Austria

Corresponding author: Klemens G. Schulmeister, Institute for Mechanic and Mechatronic, E325
Division of Control and Process Automation
Vienna University of Technology, 1040 Wien, Wiedner Hauptstraße 8-10, Austria
Email: klemens.schulmeister@tuwien.ac.at

Abstract. The object of this paper is the derivation of a model for lateral dynamics of an endless metal belt. The minimal configuration of a metal belt is a conveyor-belt over two cylindrical bend drums. In order to ensure a plane surface the metal belt is pre-stressed to a high level. The main problem of this configuration is to guarantee perfect lateral tracking of the belt utilizing swiveling drum axes, which should guarantee a constant lateral position of the belt's edges under all process disturbances and geometric imperfections. In order to design an appropriate controller a dynamic process model is derived from simple geometric parameters of the belt. Measured data from a test rig are utilized to estimate a parametric black-box model, and both analytical and experimental model are validated against experimental results. The region of validity of the linear models is evaluated and the performance of the analytical model is demonstrated.

1 Introduction

Endless metal belts are important production means for advanced processing lines with high quality demands. The product range extends from wood and laminates over casted films to food and specialty goods [1, 2, 3]. The endless metal belt is running over two cylindrical bend drums at each end of the conveyor line (one of them being the driving drum) and can be supported by a number of supporting rollers. In order to ensure a plane surface the metal belt is pre-stressed to a high level. The main problem of this configuration is to guarantee perfect tracking of the belt utilizing swiveling drum axes, which should guarantee a constant lateral position of the belt's edges under all process disturbances and geometric imperfections. In order to design an appropriate controller a dynamic process model is necessary. The output of this control loop is the lateral belt position and the control input is the swiveling angle of one drum.

Since late 1990 mathematical models for this problem have been designed which are based on the assumption that the belt acts like a beam [4]. Due to the high longitudinal pre-stress 2nd-order bending theory was employed and nonlinear models resulted as a consequence. Test rigs of different sizes have also been developed to validate this models experimentally [5]. Those models can be considered mature by now since they can reproduce measured data at a high accuracy. However, they were merely designed for the purpose to predict the lateral position of the belt off-line in the time domain [6, 7]. To this end geometric parameters of the process as well as material parameters of the belt have to be known, a friction model for the contact between belt and drums is necessary, and the transport delay for the duration of contact between belt and drum is neglected.

The model introduced in this article represents an extension for the existing model from [6, 7, 8]. This extension is threefold:

1. The transport delay of the belt on the drums is explicitly considered.
2. The number of model parameters is reduced to two simple geometric values which are known in any existing plant.
3. Due to the simple linear structure the proposed model is perfectly suited for controller design, and it can also be implemented on-line in model-based control schemes.

Although only linear relations are utilized and a purely kinematic transport on the drums is assumed, the validation using experimental data from a test rig shows a much better fit to measured data for lateral dynamics than previous models.

The remainder of this paper is structured as follows: In section 2 the model equations are derived using the static deflection of a beam and simple assumptions for the kinematic transport on the drums. In section 3 the measurement setup and the identification of a linear black-box model is described. Section 4 presents the results of the experimental validation and proves the excellent performance of the proposed model. The paper is completed by some conclusions on the main ideas and future works.

2 Modeling

The modeling approach presented here is partitioned into two parts: First, the static flexible deformation of the belt between the drums is derived from the geometric boundary conditions. Any dynamics of the elastic belt in the sense of a Timoshenko beam are neglected since these deflections are known to be orders of magnitude smaller than static deflections [9]. Second, the kinematic transport of the belt on the drums is modeled assuming perfect adhesion between belt and drum. This assumption is backed up by results from a finite element (FE) analysis [10]. The final representation of the lateral model is dependent on the belt's spatial coordinate only.

2.1 Static deflection of the free belt

Starting out from the hypothesis that the lateral belt course speed is directly proportional to the crowd angle θ in Fig. 1, the free part of the belt is modeled as a flexible beam [7]. In this case the looping part of the belt is in close contact to the drum, and each belt edge is moving on the drum like a thread on a screw conveyor.

The goal is to find an equation describing the elastic deformation of that simple beam subject to the geometric boundary conditions w_A, w_B, θ_A, and θ_B, where w_A and w_B are the lateral deflections of the bending (point A) and driving drums (point B), respectively, and θ_A and θ_B are the respective angles of the belt relative to the normal vector of the drum, see Fig. 1. The swiveling angles of the drums are denoted by β_A and β_B, and the belt's angles on the drums in absolute coordinates are given by κ_A and κ_B.

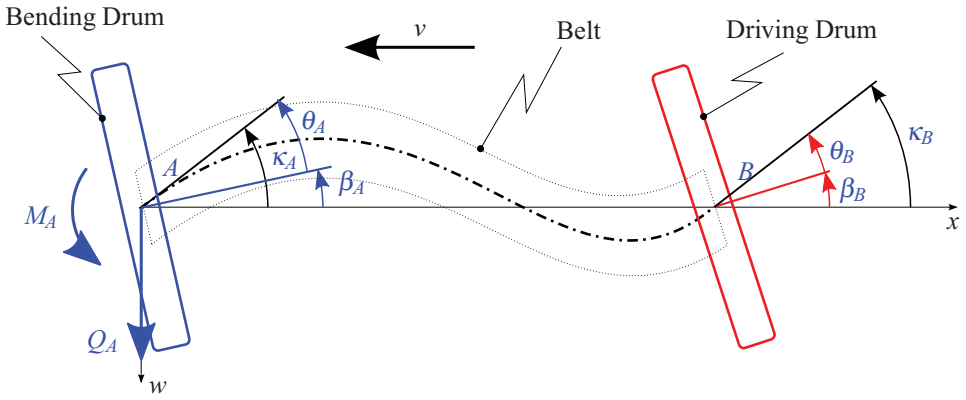

Figure 1: Sketch of the process belt modeled by an elastic beam, view of belt plane

The bending curve of a beam between the points A and B is given by an ordinary differential equation with the solution [11]:

$$\frac{d^2w(x)}{dx^2} = \frac{Q_A x + M_A}{EJ_y}, \qquad w(x) = \frac{1}{EJ_y}\left[\frac{Q_A x^3}{6} + \frac{M_A x^2}{2}\right] + C_1 x + C_2 \tag{1}$$

In (1) $w(x)$ is the beam's deflection along the longitudinal coordinate x, Q_A is the normal force at A, and M_A is the bending moment at A. Both C_1 and C_2 are integration constants and EJ_y is the bending stiffness of the belt in lateral direction.

The boundary conditions of equation (1) in A are $w(0) = w_A$ and $w'(0) = -\tan\kappa_A$, and the conditions in B at point $x = L$ are $w(L) = w_B$ and $w'(L) = -\tan\kappa_B$. Solving this system of equations and eliminating all internal forces and bending moments finally gives a general expression for the beam's deflection depending on the geometric boundary conditions.

$$w''(x) = \frac{4L-6x}{L^2}\tan\kappa_A + \frac{-6L+12x}{L^3}w_A + \frac{2L-6x}{L^2}\tan\kappa_B + \frac{-12x+6L}{L^3}w_B \tag{2}$$

which is evaluated at $x = 0$ for A and $x = L$ for B.

Linearization for small angles κ_A and κ_B leads to equations (3):

$$\tan\kappa_A \approx -w'_A, \qquad \tan\kappa_B \approx -w'_B, \tag{3}$$

and consequently, the resulting expression for the beam's deflection depending on the boundary conditions is given by

$$w''(x) = -\frac{4L-6x}{L^2}w'_A + \frac{-6L+12x}{L^3}w_A - \frac{2L-6x}{L^2}w'_B + \frac{-12x+6L}{L^3}w_B. \tag{4}$$

In eq. (4) only kinematic boundary conditions of the beam (lateral deflections and gradients) are included. As a consequence, the lateral stiffness EJ_y is no longer contained in the model.

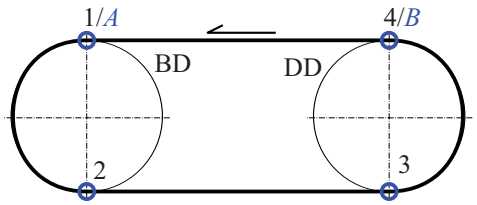

Figure 2: Numbering of the belt, *BD...bend drum, DD...driving drum*

2.2 Kinematic transport on bend drums

Assuming perfect adhesion and homogenous longitudinal stress in the belt, the lateral belt course speed $\dot{y}(t)$ on a drum is given by

$$\frac{dy(t)}{dt} = \frac{dw(x)}{dx}\frac{dx}{dt} = \frac{dw(x)}{dx}v\,, \qquad x = 0, L\,. \tag{5}$$

Equation (5) states that the edge of the belt is moving like a conveyor screw with a thread slope of $\theta = \kappa - \beta$ during stationary boundary conditions. Integration of (5) in the time domain and rearrangement yields $dy/dx = y' = dw(x)/dx$, and choosing a state vector $\boldsymbol{x}$ defined in eq. (6). The elements of $\boldsymbol{x}$ are the lateral positions y_1, y_3 and their spatial derivatives according to Figure 2.

$$\boldsymbol{x} = \begin{pmatrix} y_1' \\ y_1 \\ y_3' \\ y_3 \end{pmatrix} \tag{6}$$

The Coupling conditions between the upper belt and lower belt without transportation delay eq. (7) yields a state-space representation of the lateral dynamics.

$$\begin{aligned} y_1 &= y_2, & y_3 &= y_4 \\ y_1' &= -\kappa_1 + \beta_A, & y_2' &= -\kappa_2 - \beta_A \\ y_3' &= -\kappa_3 - \beta_B, & y_4' &= -\kappa_4 + \beta_B \end{aligned} \tag{7}$$

$$\boldsymbol{x}' = \begin{pmatrix} -\frac{4}{L} & -\frac{6}{L^2} & -\frac{2}{L} & \frac{6}{L^2} \\ 1 & 0 & 0 & 0 \\ -\frac{2}{L} & \frac{6}{L^2} & -\frac{4}{L} & -\frac{6}{L^2} \\ 0 & 0 & 1 & 0 \end{pmatrix} \boldsymbol{x} + \begin{pmatrix} \frac{4}{L} & \frac{2}{L} \\ 0 & 0 \\ -\frac{2}{L} & -\frac{4}{L} \\ 0 & 0 \end{pmatrix} \begin{pmatrix} \beta_A \\ \beta_B \end{pmatrix} \tag{8}$$

Equation (8) explicitly contains the elastic deflection of both the upper and the lower belt. The input vector to the lateral belt dynamics is given by $\boldsymbol{u} = [\beta_A\ \beta_B]^T$ which are the swiveling angles of the drums. The only and therefore dominant system parameter is the distance between the axes L. Note that (8) does not contain time as independent variable, so the model is invariant to belt transport speed v. Moreover, the longitudinal tension in the belt has not been included in the model, and for high values of pre-stress some deviations from the model have to be expected.

2.3 Transport delay

2.3.1 Geometric considerations

A speed dependent time delay is a typical characteristic of belt systems. By modeling in the spatial domain this problem is transformed in a speed-invariant transport delay which is now only due to half the drum's circumference. The belt is running around the drum in a semi-circle loop as depicted in Fig. 3, and the last point of contact between drum and belt in the upper and lower belts shows an offset of Δy.

$$\Delta y = \tan(\theta)\, R\pi \tag{9}$$

This offset can be calculated by the hypothesis of perfect adhesion between drum and belt by eq. (9). Since this offset is also present at point B, a deviation of the angle $\Delta\theta$ exists. The amount of this deviation $\Delta\theta$ depends on the distance between the axles L. So a simplification of the transport delay to zero (which corresponds to infinitesimally small drum diameters) causes an error of the crowd angle $\Delta\theta$ which is calculated in eq. (10).

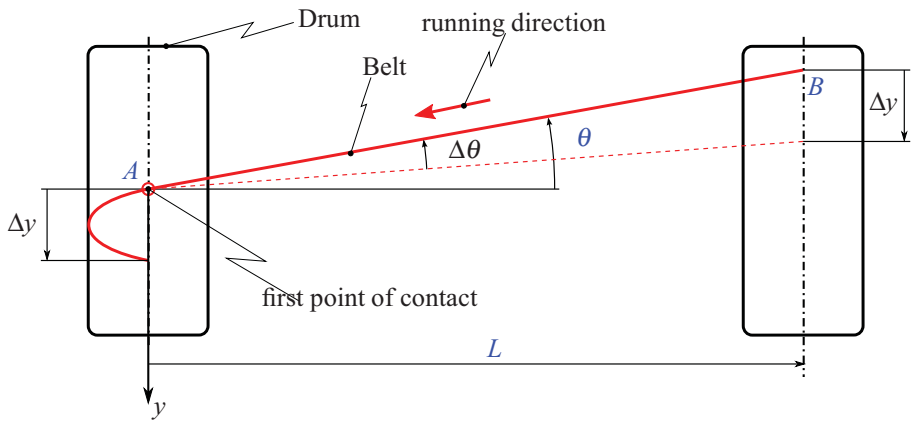

Figure 3: Error of θ as consequence of transportation simplification

$$\Delta\theta = \arctan\frac{y}{L} - \arctan\frac{y-\Delta y}{L} \approx \frac{\theta R\pi}{L} \tag{10}$$

Equation (10) allows for a calculation of a relation between angular error and angle. Using the parameters of the test rig, eq. (11) is the result:

$$\frac{\Delta\theta}{\theta} = \frac{R\pi}{L} = 0.267 \tag{11}$$

Although eq. (11) represents only an estimate which does not take into account the expiry angle of B (θ_B) it can be seen from the relation (26.7% of relative error) that the transport delay due to thread movement long the drum's surface must be considered explicitly.

2.3.2 Padé-approximation

In order to derive a linear minimum-phase model, this transport delay is approximated by a Padé-Approximation. A relative phase error e is defined similar to eq. (12), and for a given drum radius R a relationship between a relative phase error and the period length P of the belt dynamics can be represented graphically, see Fig. 4.

$$e = \frac{\varphi_{Pade} - \varphi_{Deadtime}}{\varphi_{Deadtime}} \tag{12}$$

$$P = \frac{1}{fL} \tag{13}$$

In Fig. 4 it is quite obvious that the Padé-Approximation of 1st-order (blue) already only yields an error of 3.5% at the most relevant cycle duration of L. A Padé-Approximation of 2nd-order (green) achieves an even smaller error, however, this pretended accuracy is not realistic due to other approximations.

Utilizing this approximation, a compact, linear and minimum-phase state space system with a minimum number of simple geometric parameters has been established.

3 Identification

3.1 Test rig and measurement setup

The experimental setup consists of two drums and an endless metal belt (Fig. 5). The supporting points for the bearings of the bending drum can be adjusted independently by two linear drive units. A dedicated PID-controller guarantees a constant mean longitudinal stress in the belt by synchronous adjustment of the linear units. Input to this control loop are the measured longitudinal reaction forces in the bearings. An anti-parallel adjustment of the units generates a swiveling of the drum with angle β (see Fig. 1).

The lateral position of the belt is measured at both drums. One system uses a high resolution line camera which detects the lateral position of an endless line printed onto the belt [12]. The other system is a sprung pulley pressed against the edge of the belt which is coupled to an inductive sensor.

The whole test rig is fully automated and operated via a realtime measurement and control system. All data are recorded with a sampling time of $T_s = 0.018\,\mathrm{s}$. A more detailed description of the test rig can be found in [5].

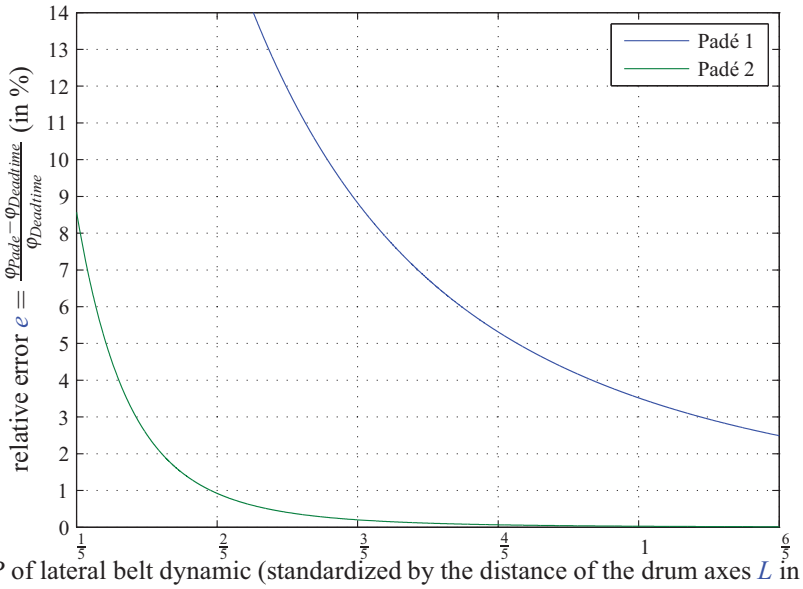

Figure 4: Relative Error of the Padé-approximation with respect to normalized belt length

Figure 5: Test rig for lateral dynamics of an endless metal belt

Each step response was recorded following the same procedure: After adjusting the swiveling drum for stationary operation stationary data were recorded for approximately 5 belt lengths L. It should be noted that the crowd angle β_0 for stationary operation is in general not $\beta_0 = 0$, since the belt's edges are not of equal length and exactly straight. This manufacturing inaccuracy leads to a constant lateral curvature of the belt during stationary operation.

A step input $\Delta\beta$ was added to the swiveling angle β_0 causing the belt to change its lateral position with constant lateral velocity after transient dynamics have decayed (integral action, see Fig. 6). The measurement was continued until the lateral position of the belt reached the operating limits.

Step responses were recorded in both directions for increasing step sizes:

$$\Delta\beta = [\pm 0.042^\circ \ \pm 0.084^\circ \ \pm 0.126^\circ \ \pm 0.168^\circ]$$

3.2 Preprocessing of measured data

Since data are originally recorded in the time domain with sample time T_s a conversion to sampling in the spatial domain with x_s and incorporating the belt speed v is necessary ($x_s = T_s v$). Since a constant sampling distance of $\Delta x = 0.1$ m is utilized for all further procedures a linear interpolation between the converted samples is performed.

Measured data from both lateral position measurements described above contain different measurement errors: Both systematic and stochastic errors are present. Additionally, outliers occur for short periods of time as can be seen in Fig. 7. The most prominent and also adverse phenomenon is the periodic lateral position error due to the manufacturing process.

Therefore, measured data were preprocessed off-line in two stages: First, the outliers were detected by an edge-detecting algorithm. The missing values were reconstructed either by interpolation or by a shift of the off-set values of the signal. In the second stage the periodic error was identified from stationary data segments and subsequently

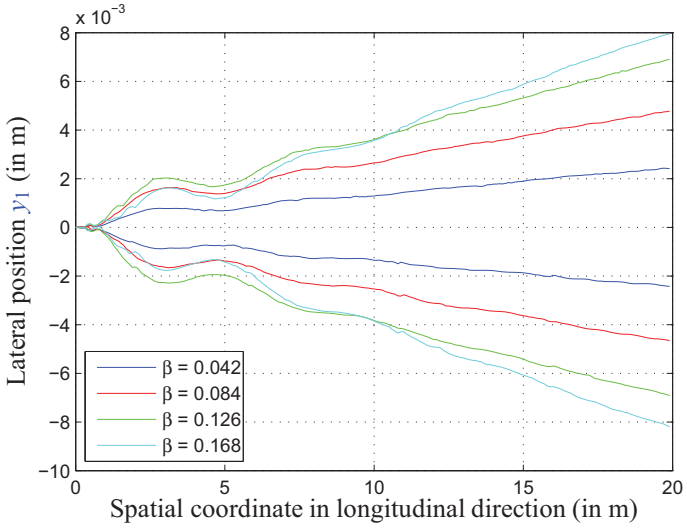

Figure 6: Measured step responses, sampling in time domain: 0.018 s, sampling in spatial domain 0.1 m

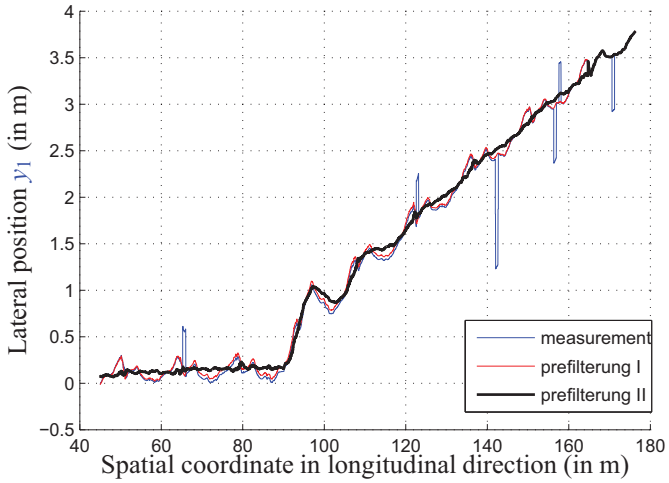

Figure 7: Measured data of step response and preprocessing

subtracted from measured data with careful adjustment of the relative phase. The original measured signal, the result after the first stage (outlier removal), and the final output signal after the second stage (removal of periodic error) can be seen in Fig. 7.

3.3 Identification procedure

Both non-parametric and parametric models have been identified from measured data using the MATLAB identification toolbox. After preprocessing of data (see section 3.2) a correlation analysis was performed in order to estimate the impulse response of the system. This non-parametric model in the time domain was also utilized for validating the system's transport delay. Additionally, a non-parametric estimate of the system's frequency response was performed (see Fig. 10).

With a fixed transport delay derived from the non-parametric models several parametric models were identified. Beginning with a 2nd-order ARX-model and utilizing ARMAX-, OE-, and Box-Jenkins-model structures with varying model orders a number of well performing models were found. Among them the best model in the sense of a good balance between simulation performance and model complexity was chosen. A 4th-order ARX-model with globally integral behavior showed best compliance with these requirements (see Figs. 8 and 10).

4 Model validation

Step responses from the experimental test rig were measured for the purpose of validation. The results of the increasing step response experiments (Fig. 6) show that symmetry of the control action is ensured. Table 1 lists the slope of the step responses and the static gain of the respective transfer function for both directions with respect to the input step size. Slope values are listed in $^{mm}/_{m}$, gain values are given in $^{mm}/_{(m\,^\circ)}$.

A 95 % confidence interval for the estimate of the mean static gain of the transfer function is therefore given by

step size $\lvert\Delta\beta\rvert$	pos. slope	neg. slope	pos. gain	neg. gain
0.042 °	0.110	-0.105	2.62	2.50
0.084 °	0.203	-0.208	2.42	2.48
0.126 °	0.320	-0.300	2.54	2.38
0.168 °	0.423	-0.425	2.52	2.53

Table 1: Stationary values for step responses with increasing step size

2.50 ± 0.062, which amounts to a relative uncertainty of 2.5 %. It is consequently safe to assume that a universal static gain of 2.5 is valid for all input step sizes. This is also a strong evidence for the assumption of linear behavior. Nevertheless, the transient behavior of the system changes for the largest step input of $\Delta\beta = \pm 0.168\,^\circ$. An additional transport delay of approximately $x_T = 0.35m$ exists, which could be due to transient slip between the belt and the drum. This obviously nonlinear phenomenon will only affect the closed-loop behavior if maximum control inputs are required.

A comparison of the different models is performed using step responses. One representative result is shown in Fig. 8. It proves an excellent agreement between measured response and the prediction from the identified model. The simple analytical model (8) exhibits a small stationary off-set but also features high accuracy for the oscillating behavior of the belt and static gain.

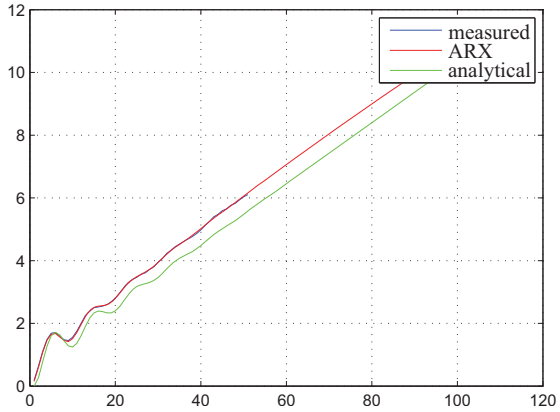

Figure 8: Step responses for lateral dynamics of the endless belt

This variation between the analytical and the identified model is more closely investigated by a pole-zero plot in Fig. 9. The dominant (close to the unit circle) poles and zeros of both models are almost identical, however, the remaining poles and zeros show considerable deviations. Nevertheless, the dynamic behavior of these models is very similar as it is confirmed by the frequency response of both systems. Bode plots from the parametric ARX-model, the analytic model, and a non-parametric estimation are shown in Fig. 10.

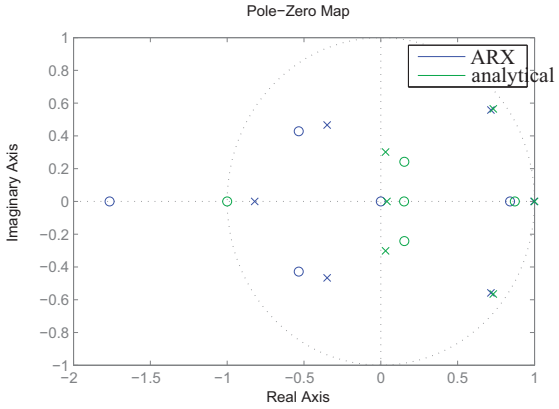

Figure 9: Pole-Zero-Map of ARX- and analytical model

An excellent agreement between these models can be seen, and only the frequency and damping of the resonance peak is slightly offset in the simple analytical model as well as a small off-set in the low frequency range exists. Again, non-parametric and parametric ARX-models show a near perfect match which indicates a good choice of the ARX-model structure.

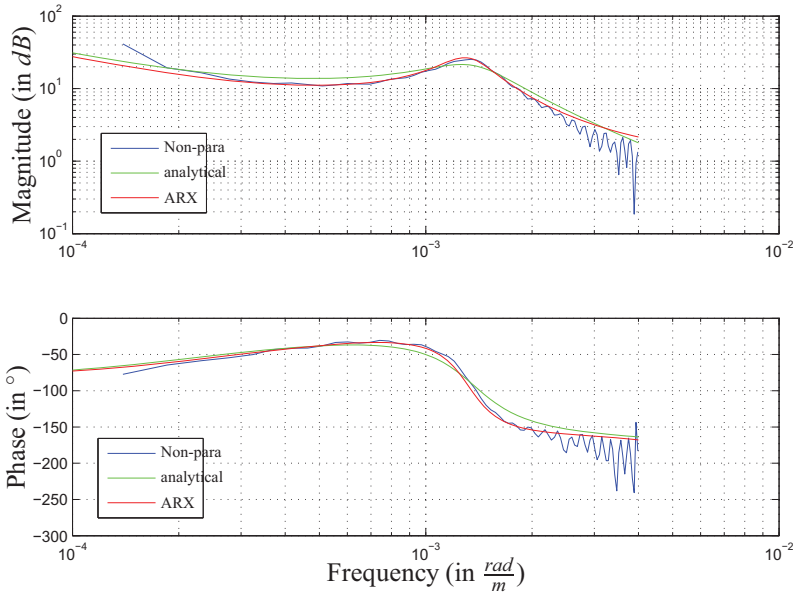

Figure 10: Bode-diagram of the models

5 Conclusion

The lateral dynamics of an endless metal belt running over two drums and controlled by a variable swiveling angle of one drum are modeled by both analytic and black-box methods. A simple analytic model which is linear, of 4th-order, and contains only two geometric parameters is presented. The transport delay of the drums is incorporated and a state space representation is given. Measurements from a test rig are utilized for identification of a an ARX-model and for validation of all models. These results clearly show that the assumption of linear system behavior is justified up to very large control inputs, where nonlinear transient behavior was documented.

It is further shown that both analytical and black-box models are consistent and capture the linearized dynamics of the process. Therefore, the presented analytical model can serve as a basis for design of a lateral position controller.

The nonlinear effects of amplitude dependent transient dynamics are topics of further research. The design of either a robust linear controller or nonlinear modifications to the control algorithm are currently under investigation.

6 Used Symbols

A	First point of contact between Bending Drum an belt
B	Last point of contact between Driving Drum an belt
β	Swiveling angle of the drum (in °)
β_A	Swiveling angle of the Bending Drum A (in °)
β_B	Swiveling angle of the Driving Drum B (in °)
e	Relative error of phase angle (in °)
E	Young's modulus of belt material (in N/m²)
f	Frquency of belt dynamic in spatial coordinates (in 1/m)
J_y	Geometrical moment of inertia, y-axis (in m^4)
κ	Constraint angle of the belt (in °)
κ_A	Constraint angle of the belt at point A (in °)
κ_B	Constraint angle of the belt at point B (in °)
L	Distance between the two drum axes (in m)
M_A	Constraint momentum at point A (in Nm)
P	Standardized periodic of lateral belt dynamic (no unit)
Q_A	Constraint shear force at point A (in Nm)
R	Radius of Drum (in m)
θ	crowd angle on overriding point (in °)
θ_A	crowd angle at Bending Drum A (in °)
θ_B	crowd angle at Bending Drum B (in °)
T_s	Sampling Time (in s)
v	Belt transport speed (in m/s)
$w(x)$	Beam deflection or lateral position of belt (in m)
w_A	Lateral position of the belt in point A (in m)

w_B	Lateral position of the belt in point B (in m)
x	Longitudinal coordinate of belt (in m)
x_s	Spatial sampling (in m)
y_1	Lateral position of the belt at point 1 (in m)
y_3	Lateral position of the belt at point 2 (in m)
y'	Rate of lateral belt position (in $^{m}/_{m}$, or as slope $^{mm}/_{m}$)

7 References

[1] Belt Technologies - Metal Belts. http://www.belttechnologies.com/conveyorbelts.htm, 2008. [online, accessed 01-Dec-2008].

[2] Berndorf Band - Steel Belts. http://www.process-belts.com/, 2008. [online, accessed 01-Dec-2008].

[3] SANDVIK. Steel Belt Book. http://www.processsystems.sandvik.com/, 1993. [online, accessed 01-Dec-2008].

[4] Martin Egger and Klaus Hoffmann. Flat Belt Conveyor. In *Proceedings of the First Cappadocia International Mechanical Engineering*. CMES, 2004.

[5] Klaus Hoffmann, Anton Pirko, and H.C. Grosz. Enhancement of Belt Conveyor Test Stand. In *Abstracts of 21st Danubia-Adria Symposium on Experimental Methods in Solid Mechanics*, 2004.

[6] Peter Ritzinger. *Seitliches Bandlaufverhalten von langsam laufenden Metallbändern auf zylindrischen Trommeln*. PhD thesis, Vienna University of Technology, May 1997. In German.

[7] Martin Egger. *Seitliches Laufverhalten des Fördergurtes beim Gurtbandförderer*. PhD thesis, Vienna University of Technology, 2000. In German.

[8] Anton Pirko. *Untersuchungen zur Gurtführung mit geregelten Schrägrollen*. PhD thesis, Vienna University of Technology, 2006. In German.

[9] Stephen Timoshenko, Donovan Harold Young, and William Weaver. *Vibration Problems in Engineering*. John Wiley and Sons, 1974.

[10] Maximilian Koller. Simulation des seitlichen Verlaufens von endlosen Stahlbändern. Master's thesis, Vienna University of Technology, 2009. In German and in press.

[11] Heinz Parkus. *Mechanik der festen Körper*. Springer-Verlag, 1995. In German.

[12] Thomas Gabmayer, Klaus Hoffmann, and Klaus Decker. Optical measuring system to acquire and control the position of running metal bands. In *24th DANUBIA-ADRIA Symposium on Developments in Experimental Mechanics*, pages 67–68, 2007.